JOURNAL OF MATERIALS SCIENCE 31 (1996) 22–30

The effect of laser surface nitriding with a spinning laser beam on the wear resistance of commercial purity titanium

H. XIN, S. MRIDHA, T. N. BAKER
Department of Metallurgy and Engineering Materials, University of Strathclyde, Glasgow G1 1XN, UK

Laser nitriding of commercial purity titanium using various concentrations of helium and nitrogen has been carried out. The surface appearance and microstructure of a treated layer were found to be dependent on the beam power density, interaction time, velocity and concentration of nitrogen. X-ray diffraction analyses have led to the conclusion that the dendrite layer in the resolidified zone of the nitrided specimens consisted mainly of TiN. The surface roughness of specimens after various laser treatments was investigated by SEM and a surface profilemeter. Using optical microscopy, the dendrite TiN and needle-like structure in the melt zone, and the large grain structure in the heat affected zone, were investigated. The surface wear resistance of nitriding CPTi was significantly improved compared to the untreated or laser glazed material, and the wear data were found to correlate with scanning electron microscopy observations. Two layers, having different microstructures, thickness and abrasive wear resistance were identified. Further, 100% overlapping considerably improved the wear resistance of the nitrided specimens.

1. Introduction

The attractive aspects of titanium materials are their excellent corrosion resistance and high strength-to-weight ratio as demonstrated in aerospace applications [1]. Unfortunately, titanium and its alloys have had a reputation for poor tribocharacteristics, but detailed information on suitable counterfaces and the wear conditions which were examined is scarce. For this reason, designers have tended to avoid the use of titanium alloys in sliding systems, but there are times when this is not possible [2–4]. There has been widespread interest in recent years in using lasers to modify surface structures and compositions, and hence to improve the wear resistance of titanium and its alloys. Laser gas alloying is used to modify the surface properties of titanium alloys through the use of gaseous interaction with the laser melted surface. Elemental titanium has a strong affinity for nitrogen. With atmospheric gases many metals form compounds such as nitrides, or oxides [5, 6]. Laser surface melting of titanium and its alloys in nitrogen to form a layer of TiN embedded in a metallic matrix which is enriched in alloying elements, has attracted considerable interest. Laser nitriding is fast and offers a flexible approach to control the composition, structure and dimensions of the processed zone [7–14]. The properties of the surface layer depend to an extent on the size and morphology of the hard material (TiN), its chemical nature and volume fraction. The amount of TiN formed is dependent on the surface to volume ratio of the melt pool, on the interaction time and the concentration of the reactive gas [11, 15]. Cracking in the nitrided layers has been identified as a major problem, although the formation of a crack-free layer was reported to be possible when the volume fraction of the TiN was kept low [12–14]. In the present work, the volume fraction of TiN was controlled by diluting the nitrogen with various concentrations of helium. Yerramareddy and Bahadur [12] have shown that laser nitriding reduced abrasive wear, while laser surface glazing did not. The reduction in the abrasive wear rate of laser nitrided specimens was attributed to the increased hardness which resulted from the formation of TiN in the molten and resolidified region. The mechanism of wear in the untreated titanium alloy was primarily ploughing. Belmondo and Castagna [16] concluded that a high wear-resistance required excellent bonding between the layer and substrate, optimum composition of the coupled materials, adequate thickness so as to ensure sufficiently long lifetimes, and the possibility of lubricant retainment. This paper outlines the characteristics and properties of an abrasive wear resistant surface developed by laser nitriding of commercial pure titanium.

2. Experimental procedure

Commercial purity titanium (CPTi) IMI 115, containing a maximum of 0.2% Fe, 0.0125% H, 0.09% O, and the remainder Ti, was used as the base alloy in this investigation. Specimens of size 80×40 mm and 3.0 mm thick were cut from the as-received material.

0022–2461

The specimens were laser surface nitrided with a CO_2 laser at AEA Culham Laboratory, Abingdon, using a 0.3 mm radius laser beam (5mm defocus distance), 5 and 10 mm s^{-1} traverse speeds, 2.8 kW laser power, a spinning beam, and various concentrations of helium and nitrogen introduced at a flow rate of 50 l mm^{-1}. The beam was spun to a diameter of 4 mm at 1500 r.p.m. The surface profiles of specimens were measured along the laser tracks using a Talysurf 5 System. To produce a standard wear specimen for a pin-on-disc type machine [16–18], 3 mm diameter cylindrical discs by 3–5 mm thick were cut from the materials and attached to a 6 mm diameter standard steel bar support using superglue. Wear tests were carried out using a constant load of 4.9 N and a speed of 0.24 m s^{-1}. The specimens were ultrasonically cleaned before testing whilst immersed in methanol, and blown dry with air before placing them in the test machine. The tests were performed against adhesively bonded P600 SiC grit paper which was replaced after every 25 m sliding. The sliding direction was kept parallel to the laser track during all tests. Weight losses were obtained after certain sliding distances, by weighting the samples to an accuracy of 10^{-5} g using an electronic microbalance. All the specimens were cleaned with methanol before and after each measurement. The tests were carried out at room temperature in air under dry conditions. Worn surfaces of materials were investigated using a scanning electron microscope. The microhardness at different depths from the surface on a vertical section was measured by a Leitz Wetzlar microhardness tester using a 100 g load. The test conditions and operational sequence of all the specimens were kept constant.

3. Results

3.1. Optical microstructure and corresponding microhardness-depth profiles

The optical microstructures and the hardness profiles of vertical-sections of the laser processed specimens are shown in Figs 1 and 2. The whole melt pool consisted of dendritic TiN and a needle-like structure, while the heat affected zone consisted of a large grain microstructure as observed in Fig. 1a. The microstructures revealed that in most cases a layer of large dendrites was formed at the surface, as seen in Fig. 1b to d. This surface layer was from 0.05 to 0.52 mm thick and the dimensions for all the specimens are given in Table I. The thickness of the layer is influenced significantly by the proportion of nitrogen used, in agreement with previous work [10]. Below the surface layer there is an intermediate zone comprised of small dendrites and needle-like structures which were reported by others as TiN and α or α' titanium [7, 8, 12, 18, 19]. The heat-affected zone produced by all these treatments consisted of a large grain microstructure. With an 80% nitrogen addition, a thin layer of large dendrites together with a thick intermediate zone were observed (Fig. 1a to e). In contrast to the 80% nitrogen addition, with a 100% addition, a thick continuous layer of dendrites with a thin intermediate zone (0.11 mm) was produced (Fig. 1f). A thick needle-like structure was formed at the intermediate zone with 5 mm s^{-1} laser traverse speed (Fig. 1b), compared with a fine needle-like structure in the intermediate zone after the faster laser traverse speed, 10 mm s^{-1} (Fig. 1c and d). In the overlapped specimen, Fig. 1e, a slightly thicker needle-like structure was observed in the intermediate zone, compared to Fig. 1c, the specimen with no overlapping. However, the microstructure in Fig. 1e is still finer than that after laser treating with the slower velocity, as seen in Fig. 1b. The maximum depth of each zone for all of the various process conditions was obtained via the hardness–depth profiles on the vertical sections, as shown in Fig. 2. From these vertical sections and the data in Table I, it is found that the depth for each of the zones decreased as the traverse velocity increased, and for the same conditions, 100% overlapping (i.e. a second pass causing a remelting of the original solidified layer) resulted in an increase in the depth of the zones. Using 10 mm s^{-1} traverse velocity, centrifical flow patterns were observed in the intermediate zone, Fig. 1c and e, but these features did not occur after 5 mm s^{-1} processing. A feature peculiar to the surface nitrided with 100% nitrogen was the formation of cracks, for example at X-Y in Fig. 1f.

The microhardness at different depths from the surface on a vertical section is also shown in Fig. 2. The maximum surface microhardness was over 2000 HV in the specimen processed with 100% nitrogen, Fig. 2d, and up to 800 HV in the specimens processed with 80% nitrogen, Fig. 2a. A slower laser traverse speed resulted in a slight increase in the microhardness of the intermediate zone (by about 30 HV), Fig. 2a and b, but the 100% overlapping technique had no effect on the microhardness of this zone. A slower laser traverse speed and 100% overlapping increased the microhardness in the large dendritic TiN layer from about 500 to 800 HV, Fig. 2a to c. Regardless of the processing conditions used, the microhardness of the heat affected zone was approximately the same as the parent material.

3.2. Scanning electron microscopy of laser nitrided surfaces and the corresponding surface roughness

The surface finish and profile graphs of materials are shown in Fig. 3 where the meter cut-off (0.8 mm) is the instrumental equivalent of the metrology sampling length. The average roughness (R_a), previously known as the Centre-Line-Average (CLA), is defined mathematically as the arithmetic average value of the departure of the profile from the centre line throughout the sampling length. R_a was read from the Talysurf 5 Systems and is given in Table II. Previous work [13–15] has shown that the nitrided surface was relatively flat and only slightly raised above the parent metal surface. The peak-to-valley height of the as-formed layers of the nitrided surface of the titanium and its alloy was at best 20 μm, compared to 5 μm in the remelted layers. In the present work, the average roughness (R_a) varied from 2.7 to 7.2 μm depending on

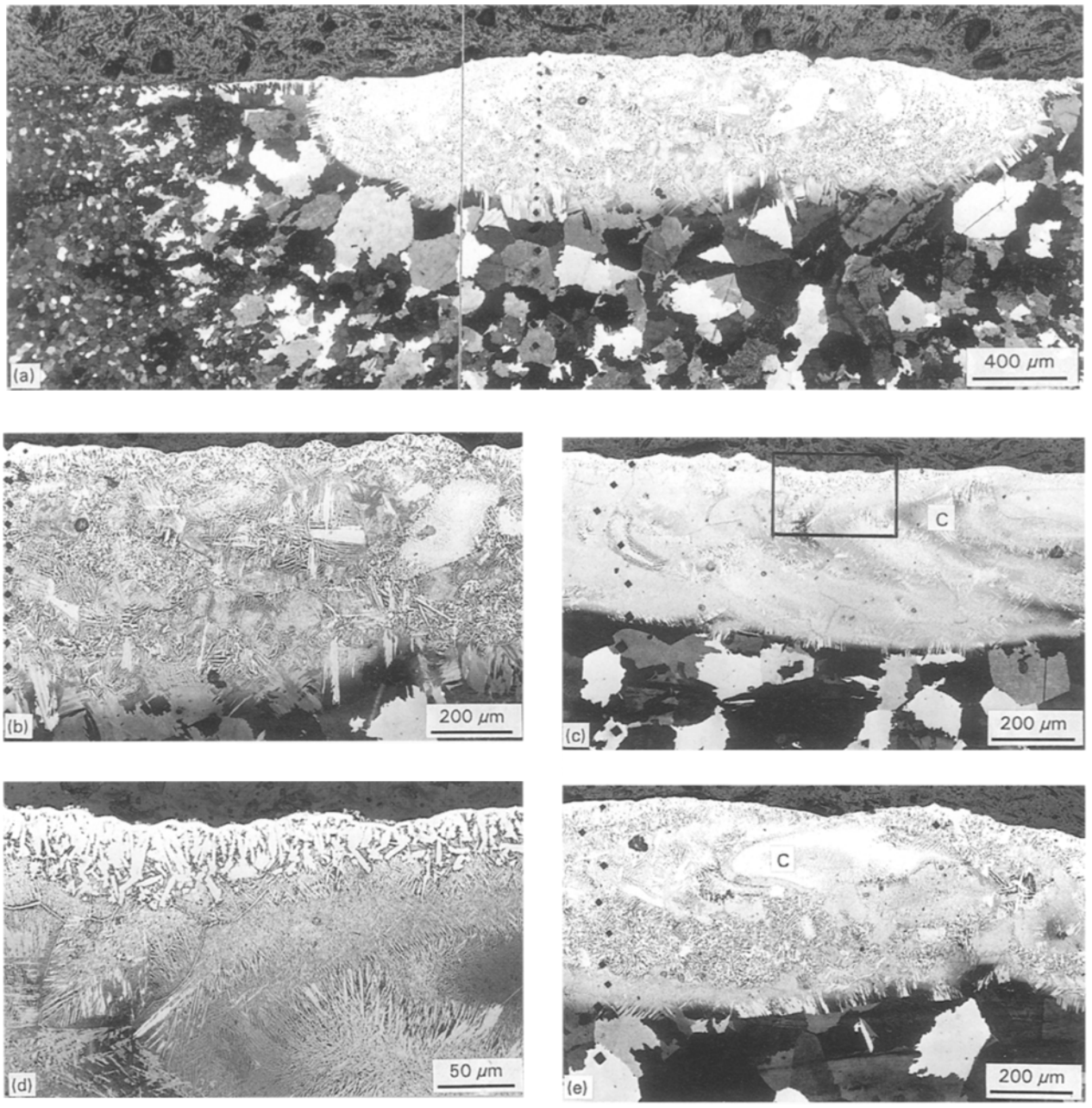

Figure 1 Optical micrographs of vertical sections through the laser processed microstructures for different laser conditions. The indentations are seen in some micrographs. (a) 2.8 kW, 5 mm s^{-1}, 80% N_2, general view. (b) as (a) with higher magnification. (c) 2.8 kW, 10 mm s^{-1}, 80% N_2, circle shows centrifical flow pattern. (d) as (c) with higher magnification showing details of the surface dendrites. (e) as (c) but with 100% overlap, circle shows centrifical flow pattern. (f) 2.8 kW, 10 mm s^{-1}, 100% N_2, showing cracks at X-Y.

the nitrogen content, traverse speed and overlapping. The peak-to-valley height is approximately 4 times R_a, which is between 11 and 29 μm. In Fig. 4, the scanning electron micrographs show the general features of the nitrided surfaces as loops and ripples, which resulted in different surface roughness measurements. A slower traverse velocity produced smaller loops; compare Fig. 4a to Fig. 4b, the specimen after the faster traverse velocity. In the overlapped specimen, Fig. 4c, slightly finer ripple marks were observed on the surface, compared to Fig. 4b, the specimen without overlapping. Rippling marks in a radial direction to the laser beam were prominent over all the surfaces observed in the specimens processed with 80% nitrogen, but not in the specimen processed with 100% nitrogen. A very smooth surface was produced in the specimen processed with 100% nitrogen, as seen in Fig. 4d which however contained pores and cracks, but these were not observed in the specimens processed with 80% nitrogen. The cracks were perpendicular to the laser beam and were observed to be connected with pores, in agreement with previous work using a stationary laser beam [13, 20].

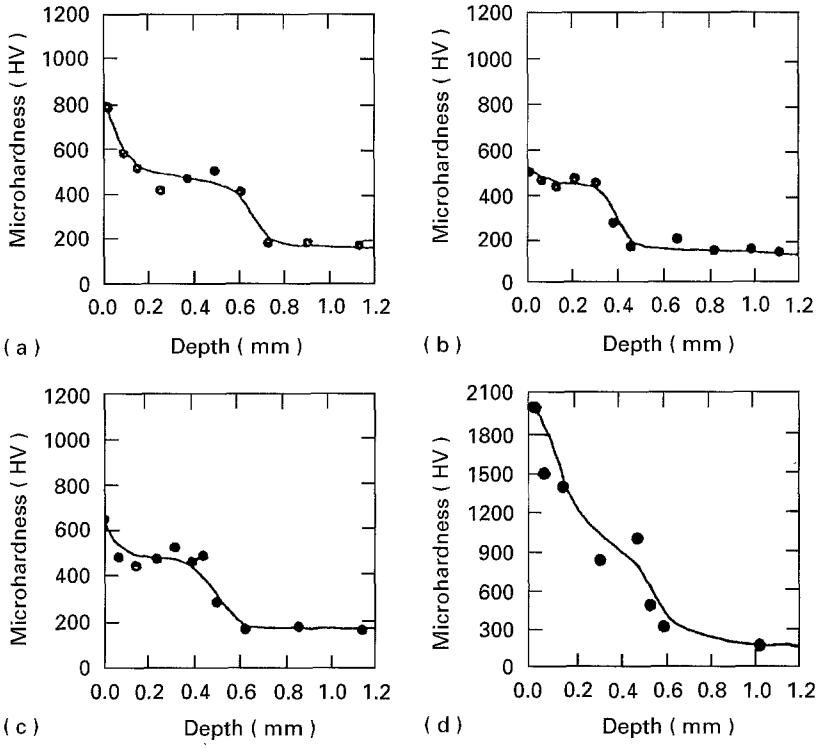

Figure 2 Microhardness–depth profiles of specimens for different laser conditions. (a) 2.8 kW, 5 mm s^{-1}, 80% N_2. (b) 2.8 kW, 10 mm s^{-1}, 80% N_2. (c) as (b) but with 100% overlap. (d) 2.8 kW, 10 mm s^{-1}, 100% N_2.

TABLE I Maximum depth of each zone

No.	Laser processing conditions	Zone of large dendrite (mm)	Intermediate zone (mm)	Heat affected zone (mm)
1	80% nitrogen, 5 mm s^{-1}	0.07	0.56	2.08
2	80% nitrogen, 10 mm s^{-1}	0.05	0.39	0.87
3	No. 2 + 100% overlapping	0.06	0.44	1.09
4	100% nitrogen, 10 mm s^{-1}	0.52	0.11	> 1.31

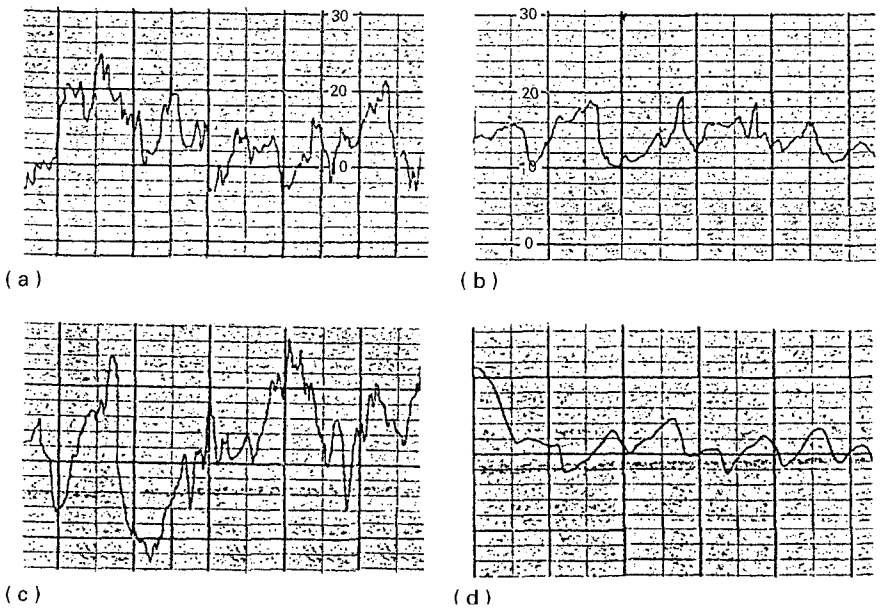

Figure 3 Surface profile graphs of specimens for different laser conditions. (a) 2.8 kW, 5 mm s^{-1}, 80% N_2 (vertical magnification × 500, 1 division = 4.0 μm). (b) 2.8 kW, 10 mm s^{-1}, 80% N_2 (vertical magnification × 200, 1 division = 10.0 μm). (c) as (b) but with 100% overlap (vertical magnification × 500, 1 division = 4.0 μm). (d) 2.8 kW, 10 mm s^{-1}, 100% N_2 (vertical magnification × 500, 1 division = 4.0 μm).

3.3. X-ray studies

Fig. 5 shows the X-ray diffraction spectra for the untreated specimen and the laser treated specimens processed with 2.8 kW, 10 mm s^{-1}, 5 mm DFD and 80%, 90%, 100% nitrogen, respectively. Obviously the peaks of α-titanium were progressively weaker as the concentrations of nitrogen increased. In the specimen processed with 80% nitrogen, Fig. 5b, the (0 1 0) and (0 0 2) peaks of α-titanium still persisted though they were very weak, and disappeared after the concentration of nitrogen increased to 90%, Fig. 5d. In contrast, the TiN peaks were progressively stronger with higher nitrogen concentrations. The X-ray diffraction analysis led to the conclusion that the region of large dendrites in the nitrided specimens consisted of TiN and α-titanium, with the quantity of TiN precipitates increasing with increasing nitrogen concentration, in agreement with previous work [12, 21]. TiN peak was not observed in the intermediate zone (0.11 mm below the surface) of the specimen processed with 80% nitrogen, Fig. 5c. This indicates that the structure is α-titanium, with nitrogen in solid solution mainly responsible for the increase in hardness.

TABLE II Average and maximum roughness of materials

No.	Laser processing conditions	R_a (μm)
1	80% nitrogen, 5 mm s^{-1}	5.4
2	80% nitrogen, 10 mm s^{-1}	7.2
3	No. 2 + 100% overlapping	3.6
4	100% nitrogen, 10 mm s^{-1}	2.7

The penetration depth of the X-rays was about 8 μm, calculated using standard methods [22]. The depth of X-ray penetration was less than one tenth of the depth of each zone shown in Table I, thereby ensuring that the X-ray diffraction spectra were not influenced by zones at greater depth with different crystal structures.

3.4. Wear resistance

The variation in abrasive wear with sliding distance for the as-received, surface-melted, and nitrided titanium specimens is shown in Fig. 6. Using the pin-on-disc test, the surface nitrided specimens showed a significant increase in the abrasive wear resistance compared to the laser melted specimen and the base material. The lowest weight loss recorded after 300 m sliding, 3.1 mg, was found in the specimen processed with 100% nitrogen, while 13.0 mg was recorded after 4.3 km sliding. The traverse velocity was found to have a significant influence on the wear resistance of the specimen nitrided with 80% nitrogen. For example, the weight loss recorded from the specimen after a velocity of 10 mm s^{-1} was twice that of the specimen processed with a velocity of 5 mm s^{-1}. Also, 100% overlapping decreased the wear rate. It can be seen that the graphs of the three specimens processed with 80% nitrogen in Fig. 6 show three slopes, described as low, medium and high. For each specimen different slopes were recorded in the low slope region, slight differences in the medium region and similar slopes to the untreated specimens in the high slope

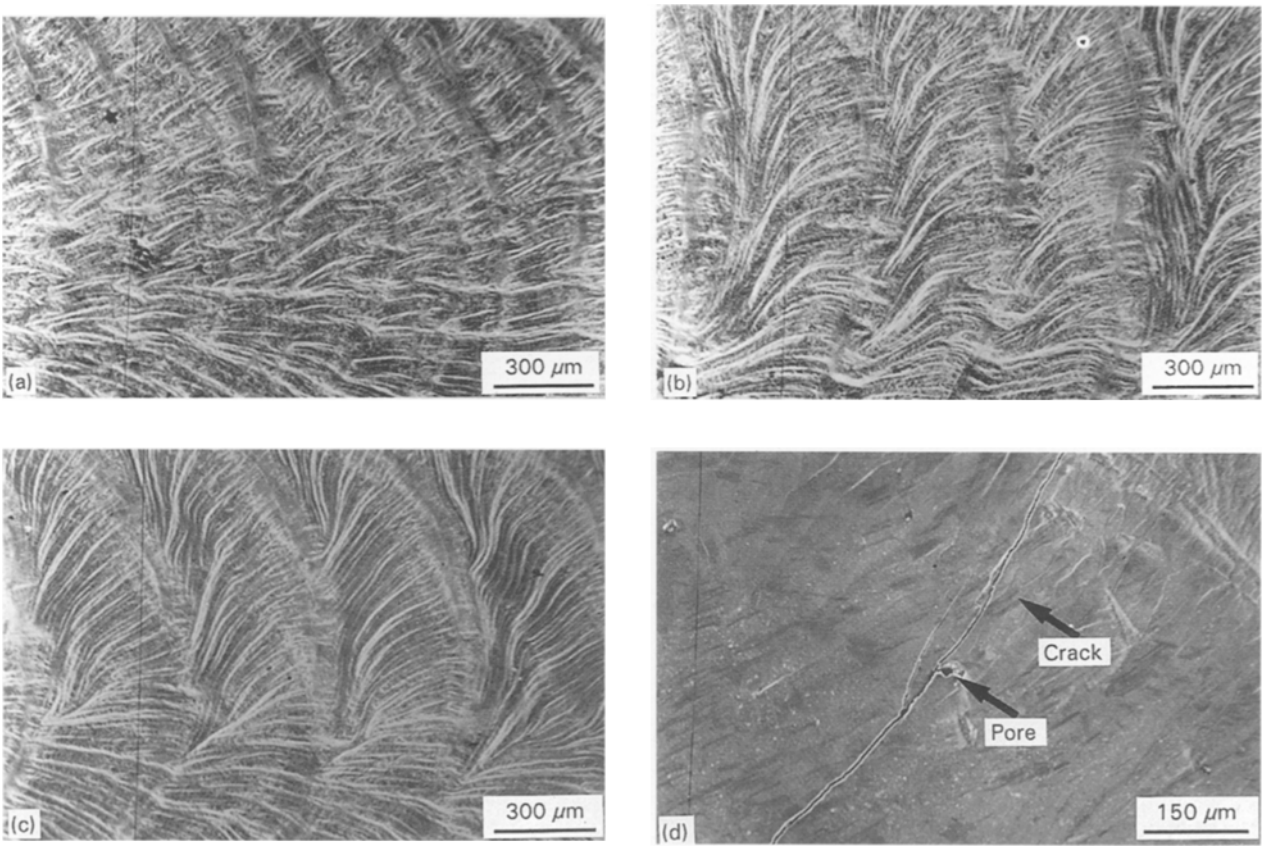

Figure 4 Scanning electron micrographs of laser nitrided surfaces. (a) 2.8 kW, 5 mm s^{-1}, 80% N_2. (b) 2.8 kW, 10 mm s^{-1}, 80% N_2. (c) as (b) but with 100% overlap. (d) 2.8 kW, 10 mm s^{-1}, 100% N_2, showing pores and cracks on the surface.

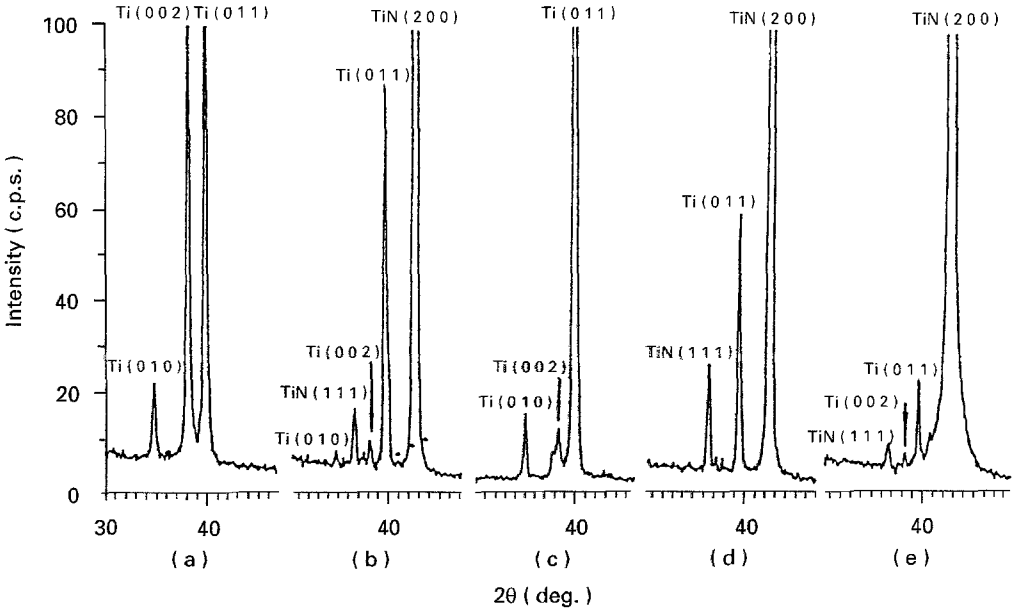

Figure 5 X-ray diffraction plots of the specimens with the laser condition 2.8 kW, 10 mm s^{-1} and different proportions of nitrogen: (a) untreated. (b) 80% N_2. (c) 0.11 mm below the surface of same specimen as (b). (d) 90% N_2. (e) 100% N_2.

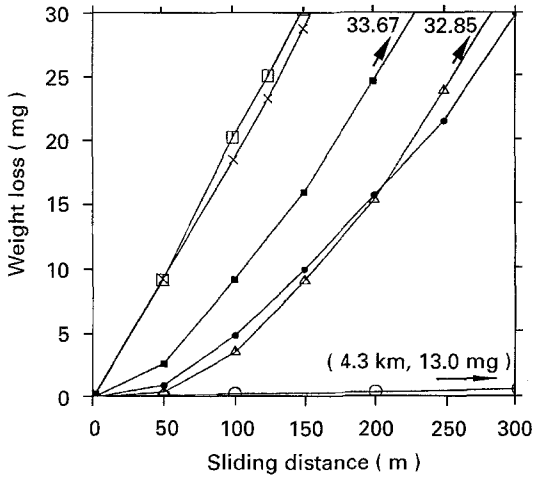

Figure 6 Weight loss of materials ground with 600 SiC grit paper (⊞ untreated; —×— under helium; —●— 5 mm s^{-1}, 80% N_2; —■— 10 mm s^{-1}, 80% N_2; —▲— 10 mm s^{-1}, 80% N_2 + overlapping; —⊖— 10 mm s^{-1}, 100% N_2).

region. It is considered that the formation of these three wear steps is related to the different layers each with different structures, formed by laser nitriding. Although the second region covered a much longer sliding distance than the first region, the wear rate was much higher, and this was related to the thicker intermediate zone compared with the thin dendrite TiN surface layer. For the 100% overlapped specimen, the first region covered only 50 m sliding distance, while the second region terminated after 200 m. Overlapping decreased the wear rate of the first region from 0.05 to 0.01 mg m^{-1}, but did not change that of the second region, which was 0.13 mg m^{-1}. Comparing the high and low traverse velocities, the latter decreased the wear rate only in the first region (from 0.05 to 0.02 mg m^{-1}) while the second region had an almost constant wear rate of 0.12 to 0.13 mg m^{-1}. The specimen processed with 100% nitrogen was tested for a total sliding distance of 5 km. This specimen showed the lowest slope on the graph, with a wear rate of 0.001 mg m^{-1} over a distance of 4.3 km. The wear rates of specimens for the as-received specimen and laser surface melted specimen under the helium were about same, 0.18 mg m^{-1}, and were also the highest.

The variation in abrasion behaviour was investigated by scanning electron microscopy and the micrographs are shown in Fig. 7. The surface morphologies of the untreated specimen and the specimen processed with 80% nitrogen and 5 mm s^{-1} traverse speed after 250 m sliding distances are shown in Fig. 7a and b. Extensive and deep plastic ploughing and cutting is seen, compared to the shallower grooves of the same specimen after 50 m sliding, Fig. 7c. The continuous ploughing and cutting grooves were not found in the specimen with 100% nitrogen even up to a sliding distance of 4.3 km. Instead, the dendritic TiN was observed to protrude from the worn surface, Fig. 7d and e, and also some pits were formed because the matrix and needle-like structures, Fig. 1d, were quickly worn away as shown in Fig. 7d. After a long sliding distance the pits increased in size and the dendritic TiN was clearly observed on the surface, Fig. 7e. Fig. 7f shows the matrix with continuous grooves where the large size dendritic TiN layer was worn away, and also an area still retaining a dispersed phase with an absence of the continuous ploughed grooves.

4. Discussion

This work used a spinning laser beam to provide a wider zone than that produced under corresponding laser processing conditions using a stationary beam. One result of this modification was that the width of the laser track produced was sufficient to allow wear testing to be carried out on a single width track, without the complications which occur after remelting part of the original track through overlapping with a second track. The laser beam was spun over a 4 mm

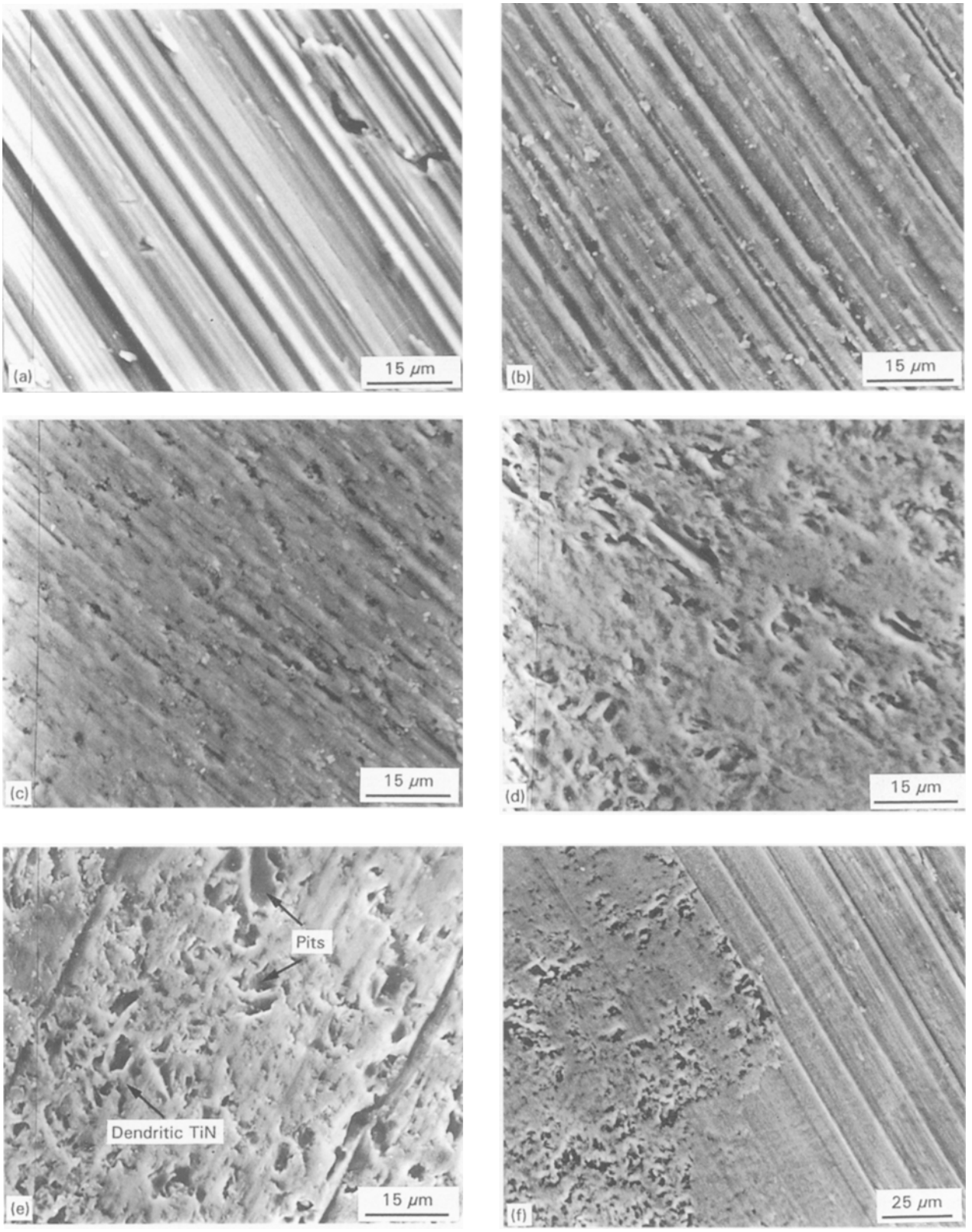

Figure 7 Worn surface of: (a) base materials, after 100 m sliding. (b) 2.8 kW, 10 mm s^{-1}, 80% N_2, after 250 m sliding, showing deep grooves. (c) as (b), but after 50 m sliding, showing shallower grooves. (d) 2.8 kW, 10 mm s^{-1}, 100% N_2, after 150 m sliding, showing plateaus and smaller pits. (e) as (d), but after 1.8 km sliding, showing plateaus and larger pits. (f) as (d), but after 1.8 km sliding, showing the area just worn away at the hard dendritic TiN layer.

diameter at 1500 r.p.m. which when superimposed on the traverse direction of the work table, produced a fine spiral track using the same laser parameters for CP titanium as those used with a stationary beam which melted a track that was too narrow to provide a specimen suitable for wear testing. A consequence of the spinning, which may give a similar result to an oscillating beam, is that the energy density is considerably lower than that obtained from a stationary beam. This reduction may have an influence on both the hardness gradient and the resistance of the laser nitrided material to cracking due to a homogenization of the heat developed in the specimen from the doughnut or annular laser profile [14].

The results of the present study showed clearly that laser surface nitriding improved the abrasive surface wear resistance of CP titanium and that a high nitrogen concentration was more effective than a low one. Surface roughening is considered to be one of the disadvantages of laser surface melting. Anthony and Cline [23] were among the first to model the fluid flow induced by radial temperature gradients that extend from the highest temperature part of the liquid to the coolest. This temperature gradient sets up a large surface-tension difference which is responsible for fluid flow from the centre of the melt towards the edges of the melt trail. Flow patterns like these have been observed experimentally using high-speed cinematography of the surface of metals [5]. In the present studies, a smoother and denser surface can be produced by nitriding in a pure nitrogen environment than by controlling the laser parameters in a dilute nitrogen atmosphere.

The different laser processing conditions produced different microstructures in the melt pool which appeared as two layers. X-ray and microscopical studies revealed that the first layer consisted mainly of large dendritic TiN and a little α-titanium, while the second layer was mainly α-titanium with nitrogen in solid solution which contributed to the microhardness, Fig. 2. This is in broad agreement with the work of Bell *et al.* [9] who reported that the microstructure of CP titanium laser melted in nitrogen was dominated by dendrites of cubic symmetry, identified by X-ray diffraction as TiN, in agreement with previous work [7, 23]. Close to the melt zone interface, Bell *et al.* found evidence of α-titanium, which has been confirmed in the present study. In the present work, the hardness of the dendritic TiN layer was found to increase from about 500 to over 2000 HV. The depth of this layer increased in the range 0.05 to 0.52 mm, with increasing nitrogen content from 80 to 100%. The hardness of the needle-like structures in the intermediate layer was about 500 HV with both a dilute and a pure nitrogen atmosphere.

The present wear test used 600 SiC grit paper as a counter face whose hardness was over 2000 HV. It is worth pointing out that the abrasion resistance experienced with the test conditions used here was directly related to the hardness. With regard to the layer hardness, Archard [24] predicted that the wear resistance of a material is proportional to the hardness. This is because the abrasion resistance was dependent on the compounds formed in the surface layers and the resistance of these compounds to abrasion. Scanning electron microscopy observations of the worn surfaces suggested the mechanisms of abrasion involved in the wear of specimens tested in this work. The protruding dendritic TiN reduced the matrix wear. In the initial period of wear, abrasive SiC particles removed the matrix and the small needle-like structures, and simultaneously started to abrade the dendritic TiN. After the matrix and small needle-like structures were removed, the exposed dendritic TiN was worn, but the abrasive wearing of the whole specimen was significantly lowered. It appears from Fig. 7c, d and e that the abrasive wearing of the surface was controlled mainly by the wear rate of the TiN dendrites and was only slightly dependent on the needle-like structures. The ploughing grooves occurred at the surface of specimens after the 80% nitrogen treatment because the hardness of SiC particles of over 2000 HV was sufficient to abrade the softer dendritic TiN surfaces (from 500 to 800 HV). When the concentration of nitrogen increased to 100%, the hardness of the dendritic layer increased to 2000 HV, Fig. 2d. As a result, the SiC particles were no longer able to readily abrade this dendritic TiN surface, so that the ploughing grooves were not found on this worn surface. Instead, the dendritic TiN which protruded from the worn surface after the initial wear controlled the wear rate. When the wear debris increased, they accumulated among the dendritic TiN, which resulted in a faster wear rate through the formation of pits. Fig. 7e showed clearly the dendritic TiN left, which protruded on the surface after 1.8 km sliding. It is clear that the wear rate of the specimen processed with 100% nitrogen was superior to all other specimens tested in this work, despite the presence of cracks and pores. However, these defects would be expected to have a significant influence on erosion wear resistance.

5. Conclusions

1. Microstructural studies and X-ray diffraction analyses of CO_2 laser nitrided IMI 115 CPTi specimens have shown that the melt zone consisted of the continuous TiN layer followed by dendritic TiN and then needle-like structures in an intermediate layer where TiN was not detected by X-ray diffraction. The hardness of the dendritic TiN layer was dependent on the concentration of nitrogen in the nitriding atmosphere. The depth of the dendritic TiN layer decreased by an order of magnitude when the nitrogen concentration was reduced from 100 to 80%.

2. 100% overlapping of the layer tracks in the 80% nitrogen laser processed specimens increased the hardness of the dendritic TiN layer from about 500 to 650 HV, but did not affect the hardness of the intermediate layer.

3. The slower laser traverse velocity of 10 mm s^{-1} compared to 5 mm s^{-1} also increased the hardness of the dendritic TiN layer, but did not significantly affect the intermediate layer.

4. Laser surface nitriding of commercial pure titanium significantly improved the wear resistance. Two major changes in wear rate were identified and shown to be due to differing microstructures. When these layers were completely abraded, the wear rate became that of the untreated alloy. The specimen nitrided under 100% nitrogen content produced the lowest wear rate of 0.001 mg m^{-1} which was maintained for a test of 4.3 km sliding distance, but the laser nitrided surface contained cracks.

Acknowledgements

Thanks are due to MOD/RAE and Imperial Metals Industries for the gift of materials, to Dr C. F. Burdett for helpful discussions during the X-ray investigation

and to Dr J. H. P. C. Megaw and his staff of the Beam Science and Technology Department of AEA Technology, for advice on laser processing. One author (H. X.) gratefully acknowledges the support of an ORS award.

References

1. I. J. POLMEAR, "Light Alloys, The Metallurgy of the Light Metals" (2nd edn), (Edward Arnold, 1989) pp. 265–268.
2. P. H. MORTON and T. BELL, Proceedings of the 6th World Conference on Titanium, Cannes, 1988, edited by P. Lacombe, R. Tricot and G. Beranger (Les Editions de Physique, Paris, 1988) pp. 1705–1712.
3. F. M. KUSTAS and M. S. MISRA, "ASM Handbook, Friction, Lubrication and Wear Technology", Vol. 18 (American Society for Metals, Metals Park, Ohio, 1992) pp. 778–784.
4. K. G. BUDINSKI, *Wear* **151** (1991) 203.
5. C. W. DRAPER and J. M. POATE, *Int. Met. Rev.* **30** (1985) 2, 85.
6. C. TANG, H. ZHAO, W. FENG, H. ZHENG, *Heat Treatment of Metals* **10** (1990) 52.
7. S. KATAYAMA, A. MATSUNAWA, A. MORIMOTO, S. ISHIMOTO and Y. AVATA, Proceedings of the International Conference on Applied Laser Electro-optics 1983, edited by E. A. Metzbower (Laser Institute of America) pp. 127–134.
8. J. A. FOLKS, P. HENRY, K. LIPSCOMBE, W. M. STEEN and D. R. F. WEST, Proceedings of 5th International Conference on Titanium (1984) pp. 987–994.
9. T. BELL, H. W. BERGMANN, J. LANAGAN, P. H. MORTON and A. M. STAINES, *Surf. Eng.* **2** (1986) 133.
10. M. S. OSLO, Proceedings of 2nd European Conference on Laser Treatment of Materials (ECLAT), DVS berichte Vol. 113 (1988) pp. 66–69.
11. S. Z. LEE and H. W. BERGMANN, Proceedings of the 6th World Conference on Titanium, Cannes, 1988, edited by P. Lacombe, R. Tricot and G. Beranger (Les Editions de Physique, Paris, 1988) pp. 1811–1816.
12. S. YERRAMAREDDY and S. BAHADUR, *Wear* **157** (1992) 245.
13. V. M. WEERASIHGE, D. R. F. WEST and M. CZAJLIK, *Mater. Sci. Forum* **102–104** (1992) 401.
14. S. MRIDHA and T. N. BAKER, *Mater. Sci. Eng.* **A188** (1994) 229.
15. H. S. UBHI, T. N. BAKER, P. HOLDWAY and A. W. BOWEN, Proceedings of the 6th World Conference on Titanium, Cannes, 1988 edited by P. Lacombe, R. Tricot and G. Beranger (Les Editions de Physique, Paris, 1988) pp. 1687–1691.
16. A. BELMONDO and M. CASTAGNA, *Thin Solid Films* **64** (1979) 249.
17. R. HUTCHINGS and W. C. OLIVER, *Wear* **92** (1983) 1443.
18. S. ATAMERT and H. K. D. H. BHADESHIA, *Metall. Trans. A* **20A** (1989) 1037.
19. A. WALKER, J. A. FOLKS, W. STEEN and D. R. F. WEST, *Surf. Eng.* **1** (1985) 23.
20. S. MRIDHA and T. N. BAKER, *Mater. Sci. Eng.* **A142** (1991) 115.
21. B. L. MORDIKE, Proceedings of 2nd European Conference on Laser Treatment of Materials (ECLAT) DVS berichte Vol. 113 (1988) pp. 389–413.
22. C. S. BARRETT, "Structure of Metals", 2nd Edn (McGraw-Hill Book Co., New York, 1953) pp. 54–56.
23. T. R. ANTHONY and H. E. CLINE, *J. Appl. Phys.* **48** (1977) 3888.
24. J. F. ARCHARD, *ibid.* **24** (1953) 981.

Received 14 June
and accepted 17 July 1995